AN LS-DYNA USER DEFINED MATERIAL MODEL FOR LOOSELY WOVEN FABRIC WITH NON-ORTHOGONAL VARYING WEFT AND WARP ANGLE

Marlin Brueggert
Romil R. Tanov
Center for Advanced Product Evaluation, Division of IMMI
18881 US 31 North
Westfield, Indiana 46074-1020

ABSTRACT

The behavior of loosely woven fabrics (LWF) differs significantly from other types of woven fabric materials, the major difference being the significant change that the angle between the weft and warp fibers undergoes as the fabric stretching forces change. These unique characteristics have made the LWF a very important part for the functionality of some recently developed occupant protection safety devices for the automotive and heavy machine and truck industry. To efficiently model and analyze the behavior of such devices within an occupant protection model, an accurate representation of the characteristics of the LWF is needed. However, none of the many available LS-DYNA material models seem to fit well with the unique kinematics of the LWF. Therefore, the aim of this work is to present the basics of a formulation for a material model for the analysis of LWF and its implementation as a user defined material in LS-DYNA. To assess the performance of the model, results from the simulation are presented. Although relatively simple, the developed model seems to represent very well the behavior of the LWF and the simplicity of the formulation attributes to the efficiency and stability of the user defined material subroutine.

Corresponding Author:
Marlin Brueggert
CAPE, A Division of IMMI
18881 US 31 North
P.O.Box 1020
Westfield, IN 46074-1020
Phone: (317) 867-8273
Fax: (317) 867-2305
E-mail: crashsim@iquest.net

Abbreviations: FE   finite element
                  ITS   inflatable tubular structure
                  LWF   loosely woven fabrics
                  RC   representative cell

INTRODUCTION

Woven fabric generally consists of two interlaced sets of yarns at right angles to each other. Depending on the gaps between the adjacent parallel yarns, woven fabrics can be characterized as tightly woven or loosely woven, the former having smaller gaps or no gaps at all. The gap width can significantly affect some of the characteristics of the fabric making it suitable for different uses. Due to the wide gaps between the fibers, loosely woven fabric is capable of undergoing very large in-plane deformation when it is subjected to varying in-plane loading (see Fig. 1). This unique characteristic has been successfully utilized in the design of a recently developed side-impact occupant restraint system. In normal operation the inflatable device is hidden in the form of a long thin tube usually in the vehicle body. In an accident the tube expands radially and shrinks significantly in its axial direction, which forces it to position itself between the occupant head and the door thus providing the necessary head and neck protection. The braided fabric layer used in the device provides significant shrinkage in one direction while being pulled along the perpendicular direction. In that process the directions of the fibers constituting the fabric and the angle between them change in a wide range. This change is so significant that a piece of that fabric would act like a mechanism rather than a continuous medium. To be able to efficiently implement this inflatable side airbag into newly developed vehicles one has to be able to accurately model its behavior including inflation, deformation, and interaction with the vehicle body and occupant. Such modeling calls for a powerful transient dynamics finite element code as LS-DYNA (Hallquist, 1998). Since the inflatable side airbag incorporates a bladder made of a more conventional airbag fabric and is inflated with an airbag inflator, its inflation process can be successfully modeled using the LS-DYNA airbag inflation models. Furthermore, the contacts between the loosely woven fabric and the bladder, vehicle trim and interior, and occupant can be efficiently handled by the code contact definitions. And the fast speed of the inflation process itself calls for an explicit analysis with a fine resolution within the time domain. However, it is impossible to successfully model the behavior of the LWF layer using any of the existing LS-DYNA material models for fabrics or other continua. This is primarily due to the fact that to be able to approximate the deformation of the LWF fiber mechanism a material model would have to implement varying material Poisson's
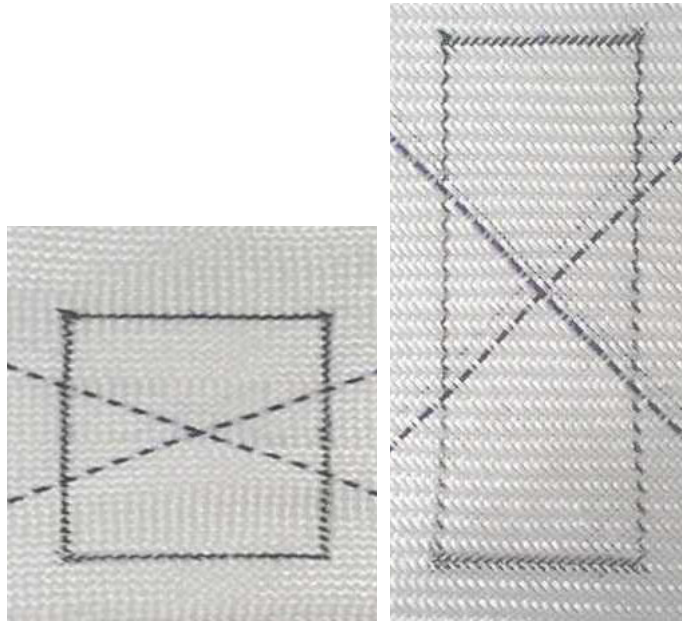
Figure 1. The Loosely Woven Fabric at 40° and 90° Angle Between Fibers

ratio with a wide range of variation: from close to zero, up to more than unity. It is obvious that this is beyond the capabilities of the currently implemented FE material models. To be able to analyze the LWF layer a new constitutive formulation has to be defined and incorporated into the code. Therefore, the aim of the present work is to define a mathematical formulation representing the constitutive relations for the fabric and program this

formulation as a user defined material model in LS-DYNA. The basics of the formulation and the FE implementation are herein presented, as well as some validation examples and results compared to test data.

THE LOOSELY WOVEN FABRIC MODEL

The theoretical formulation of the LWF constitutive model is based on a micromechanical approach utilizing the Representative Cell (RC) concept. Starting from a portion of a LWF layer, Fig. 2, we consider a repetitive volume of the fabric layer and assume that this volume is representative of the constitutive characteristics of the whole fabric. This volume we call the RC as shown on Fig. 2. The RC approach has been widely used in various woven fabrics
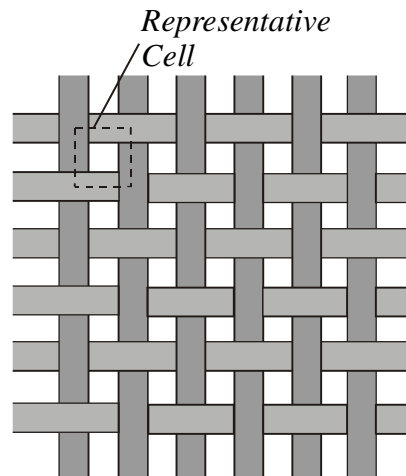
Figure 2. The Loosely Woven Fabric Layer and a Representative Cell

constitutive models. However, existing formulations (e.g. see Ishikawa and Chou 1982, Naik and Ganesh 1995, Whitcomb et al. 1995, Tabiei et al 2000, Tanov and Tabiei 2001) will not work for the LWF because none of them takes into consideration the in-plane angle change between the fibers in the deformation process. A fabric model that takes into account the yarn angle change is implemented into the FE portion of the Madymo analysis code (see TNO Automotive 1999). This model seems to have been successfully used (Meister and Steenbrink 1999) to model the behavior of a very similar Inflatable Tubular Structure (ITS) in a passenger car. However, this model does not account for the interlocking of the fiber yarns as the angle between them decreases. This interlocking changes significantly the behavior of the LWF layer, it is an important phenomenon in the LWF constitutive response, and is even more important if we have to model the ITS in cases where the vehicle cab geometry results in a higher axial shrinkage requirement (e.g. commercial, off-highway, and construction vehicles).

a)   *b)*
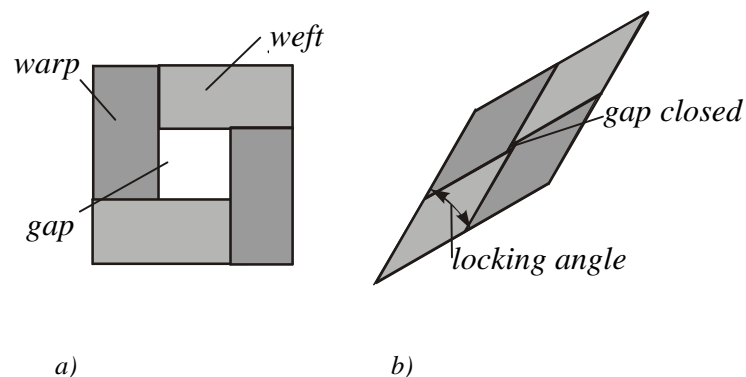
Figure 3. The Representative Cell with Orthogonal (a), and Locked (b) Fibers

As seen on Fig. 3.a in LWF there is a significant gap enclosed between the two warp and two weft fibers of the RC. Since the fibers can rotate almost freely, prior to closing the gap, the RC behaves more like a mechanism, which can be represented with a simple truss system of four rods connected with hinge joints. The reaction forces at the four hinge nodes will only be due to the stretching of the fiber bars. As the mechanism deforms, the angles change and eventually the gap between the fibers closes, Fig. 3.b. Then, the fibers lock and the behavior of the RC changes: additional nodal forces appear due to the transverse compression of the fibers as they squeeze together. This behavior can be efficiently modeled using the simple mechanism presented in Fig. 4. In addition to the four bars

along the sides of the RC it has two springs along the diagonals, which purpose is to model the locking mechanism in the LWF behavior. The springs have stiffness, which changes with the change of the angle between the warp and weft fibers. They have zero stiffness prior to locking, and as locking initiates their stiffness gradually increases from zero to its final value (see Fig. 5).
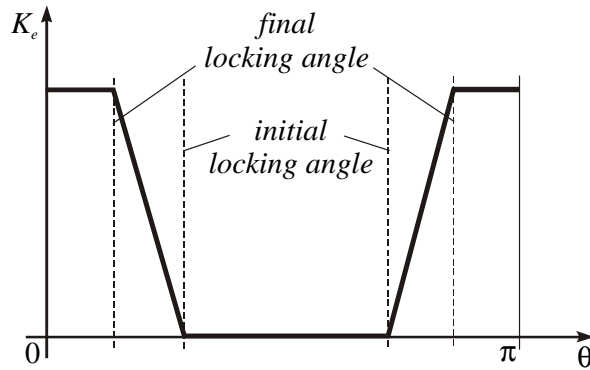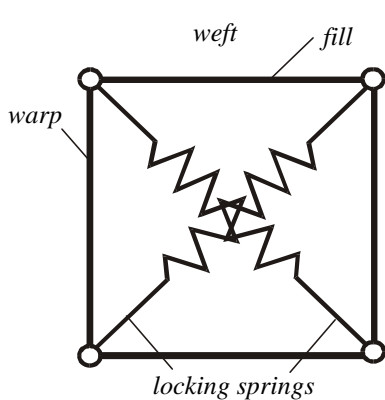
Figure 4. The Model of the RC   Figure 5. Locking Springs Stiffness, K_e, Versus Angle between Fibers, θ

To implement the model in Figs. 4 and 5 into the FE analysis scheme an LS-DYNA user defined material model was developed. The model requires as input the values of the weft and warp fibers modulus of elasticity, the initial angle between the fibers, the initial and final locking angle (see Fig. 5), and the elasticity modulus of the locked fabric. Some model parameters are stored in history variables and can be viewed at the post-processing stage. These are: the angles of the two fibers with respect to the local x-axis; the fiber projections along the local x- and y-axis; the components of the displacement gradient (see Eqs. 4 and 5); and the axial stresses in the two fibers.

User Defined Subroutine Steps
Incremental Strain Method. In the standard explicit scheme of finite element analysis, the strain increments at the current time step are related to the stress increments by the material constitutive model. The stresses are then used to assemble the force vector for the next increment in the solution by the central difference time integration. The subject LWF material behaves like a plane stress membrane. Accordingly, the corresponding strain increments in the plane of the element are described by the incremental strains arranged in a vector:

$$\Delta \boldsymbol{\varepsilon} = \left\lfloor \Delta \varepsilon_x \quad \Delta \varepsilon_y \quad \Delta \varepsilon_{xy} \right\rfloor^T \tag{1}$$

Outline of General Approach. The incremental strain-stress approach described above requires, at least for the LWF material,

1) fiber stretches (λ_1 and λ_2) from which the fiber stress-strain relationship is used to determine fiber stress, and
2) tracking of fiber re-orientation to properly relate fiber stresses to element local stresses.

Knowing the fiber directions $\mathbf{n}_1$ and $\mathbf{n}_2$, the fiber stretches λ_1 and λ_2 can be calculated from the right Cauchy-Green deformation tensor $\mathbf{C}$ as (see Ch. 6.2.2 of Bathe 1996)

$$\lambda_i = \left(\mathbf{n}_i^T \mathbf{C} \mathbf{n}_i \right)^{\frac{1}{2}} \tag{2}$$

where $\mathbf{n}_i$ is a vector of direction cosines of fiber i at time zero. Both the fiber orientations and these direction cosines are calculated from the principal stretches and right Cauchy-Green deformation tensor as

$$\cos \alpha_i = \frac{\mathbf{n}_i^T \mathbf{C} \mathbf{e}_1}{\lambda_i \lambda_e} \tag{3}$$

where $\mathbf{e}_1 = [\, 1 \; 0 \,]^T$ is the local x-axis unit vector and $\lambda_e = (C_{11})^{1/2}$.

Subroutine Implementation. Computation of the right Cauchy-Green deformation tensor is fundamental to the method of implementation. In the first pass through the subroutine, the history variables for fiber angles, projections, displacement gradients, and stresses are initialized. On subsequent calls to the subroutine, the displacement gradient is incremented by the incremental strains:

$$\Delta \mathbf{G} = \begin{bmatrix} \Delta \varepsilon_x & \Delta \varepsilon_{xy} \\ \Delta \varepsilon_{xy} & \Delta \varepsilon_y \end{bmatrix} \tag{4}$$

$$\mathbf{G}^n = \mathbf{G}^{n-1} + \Delta \mathbf{G}^n \tag{5}$$

The displacement gradient is transformed to the deformation gradient $\mathbf{F}$ by

$$\mathbf{F} = \mathbf{G} + \mathbf{I} \tag{6}$$

where $\mathbf{I}$ is the identity matrix.

The right Cauchy-Green deformation tensor $\mathbf{C}$ is related to the deformation gradient $\mathbf{F}$ by

$$\mathbf{C} = \mathbf{F}^T \mathbf{F} \tag{7}$$

The fiber stretches λ_i are calculated at this point, then the fiber angles are updated. From the fiber stretches and the user-provided stress-strain relation, the stress increments in the fibers (fiber directions) are calculated from

$$\Delta \sigma_i = E \, (\lambda_i - 1) \tag{8}$$

where E is the user provided modulus. The incremental fiber stresses are transformed to the shell element coordinate system and then the element stresses are incremented and stored in the appropriate history variables.

The existence of locking is checked, based on the scheme of the aforementioned unit cell and lattice model and the updated fiber angles. The angle between fibers is calculated and if it is less than the material-defined lock angle, locking begins if the lock spring is in compression. The angle at which locking starts and the angle at which it is fully achieved is obtained from material tests and input by the user as a material property. The locking is fully implemented over several cycles and determined by stability limits. Locking stresses are transformed to the element coordinate system and the element stresses are incremented by the locking stress.

The element in-plane shear stress had to be dampened for stability reasons. The shear stress damping is a heuristic concept, the existence of which is based on friction between fibers in the fabric as they move across each other. The shear-damping factor was empirically determined from component tests of the real, inflated structures of LWF.

DISCUSSION OF RESULTS

The implemented new material model is used in LS-DYNA to investigate the behavior of an inflatable occupant protection system. The constitutive model is combined with a membrane element formulation. Experiments showed that a membrane element with full integration performs much better with the LWF material model than the

uniformly underintegrated membrane. Specifically, we obtained the best results with LS-DYNA Type 9 membranes.

For its computations the developed material model needs at input the values of the following model parameters: modulus of elasticity of the fibers constituting the LWF, E_f; the initial angle between the two fiber directions, α_0; the initial locking angle, α_{li} (see Fig. 5); the final locking angle, α_{lf} (see Fig. 5); and the locking spring stiffness, K_e. These values were determined from tests performed on LWF specimens, and for the fabric used they were found to be: $E_f = 2 \times 10^8$ Pa; $\alpha_0 = 46°$; $\alpha_{li} = 38°$; $\alpha_{lf} = 32°$; and $K_e = 2 \times 10^8$ Pa. Note that the locking spring stiffness has dimensions of force/area and it directly relates the stresses to the corresponding strains after locking. The LWF material modeled has density of 724 kg/m^3.

Single Element Example
Case 1: No Locking. The results from a single element LWF model are presented herein to illustrate the performance of the LWF formulation and its subroutine implementation. The model consists of a single planar rectangular
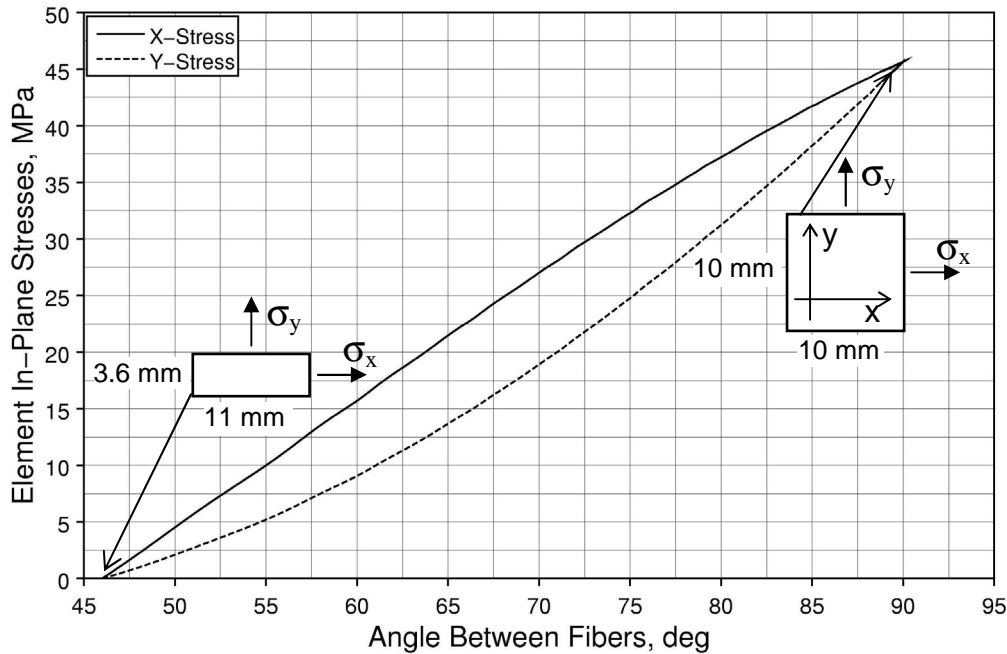
Figure 6. Stresses in a Single Element Example

element with dimensions of 11 *mm* in the *x*-direction and 3.6 *mm* in the *y*-direction. These dimensions are chosen so as to make the weft and warp fibers be oriented along the element diagonals for purely illustrative purposes. The element is pulled along the *y*-axis and can shrink or expand in both *x*- and *y*-directions. All four nodes have attached springs acting along the *x*-axis to balance the external loading. The model starts with weft and warp fibers at ±23° with respect to the *x*-axis and is loaded until the fibers become orthogonal. Results for the *x*- and *y*- stresses are presented on Fig. 6 plotted versus the angle between the weft and warp fibers. As seen from the figure, as the element deforms the two stress components are different but when the angle reaches 90° the stresses become equal and the element becomes a square.

Case 2: Locking Mechanism Engaged. To illustrate the function of the locking mechanism incorporated into the LWF constitutive model, the same example is modified by interchanging the directions of the load and springs: the load acts in the *x*- and the springs in the *y*-direction. Also, the spring stiffness is reduced to produce very small reaction forces in the mechanism prior to locking. The results for the stress variation as the angle decreases are shown in Fig. 7. As seen, prior to locking, there are practically zero stresses in both directions. Once the locking mechanism is engaged, the stress in that direction rapidly increases to oppose the external loading, while the stress in the *y*-direction remains unchanged and very small. After locking the element behaves like an elastic material with prescribed elastic modulus and varying Poisson's ratio depending on the fiber angle change.
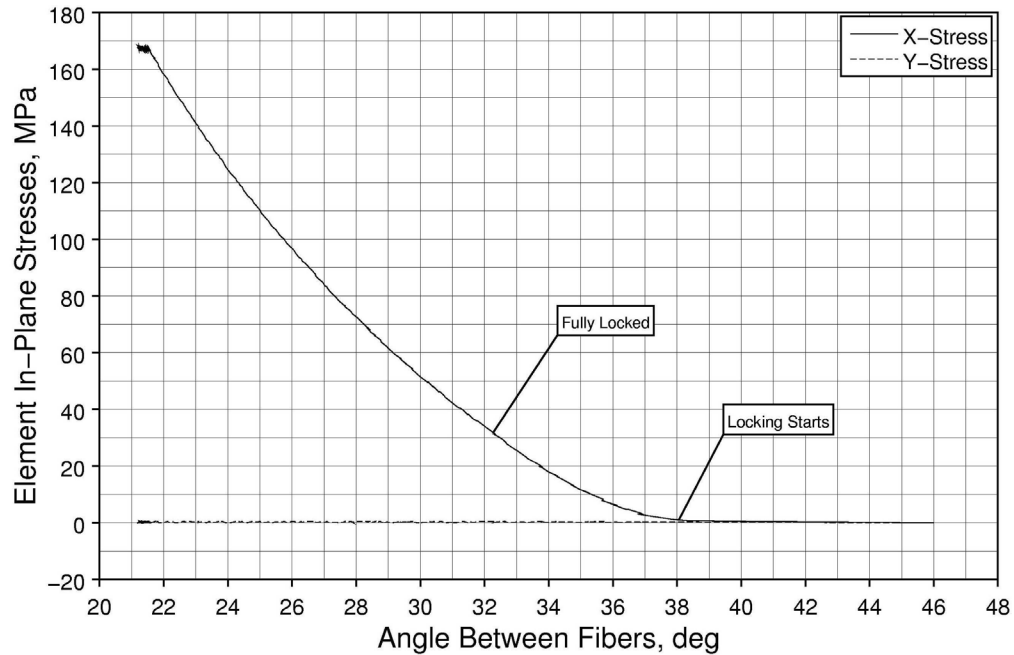
Figure 7. Stresses at Fiber Locking in a Single Element Example

Side Airbag Example
Results from the FE analysis are compared herein to results from a test deployment of an inflatable protection system. The FE model is created to represent both the outer LWF layer and the inner fabric airbag bladder, the latter represented by a standard fabric material model available in LS-DYNA. Within the FE model both inner and outer bags are folded following the folding pattern of the actual system. The inflation process is represented using a simple airbag model available in LS-DYNA. The inflation is controlled by a prescribed mass flow rate into the airbag chamber. This mass flow rate is determined using the laws of thermodynamics and based on the characteristics of the inflator used in the inflation process. The pressure decay due to the gas flowing out through the airbag fabric is modeled by prescribing an exit vent, the area of which depends on the current airbag pressure. This leaking mechanism is assumed to be a characteristic of the whole airbag.
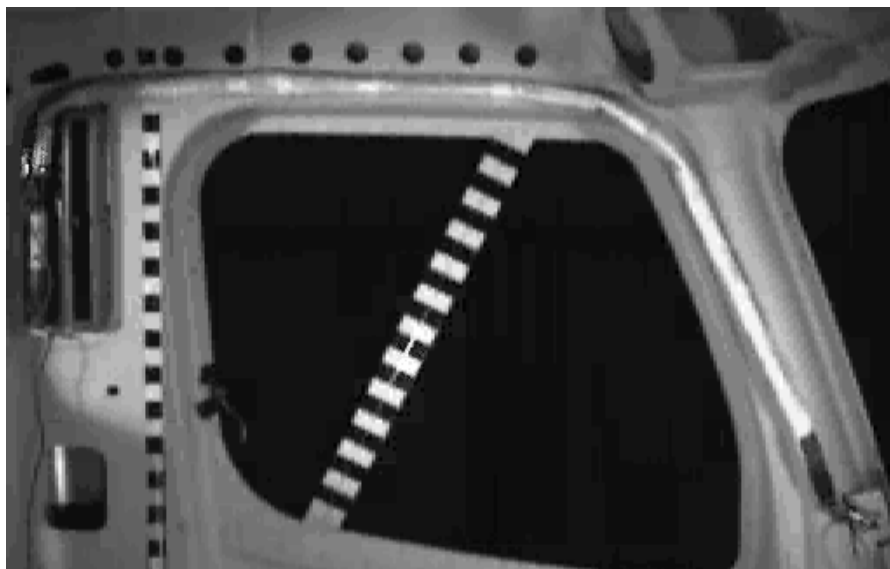
Figure 8. Test and FE Analysis before Inflation
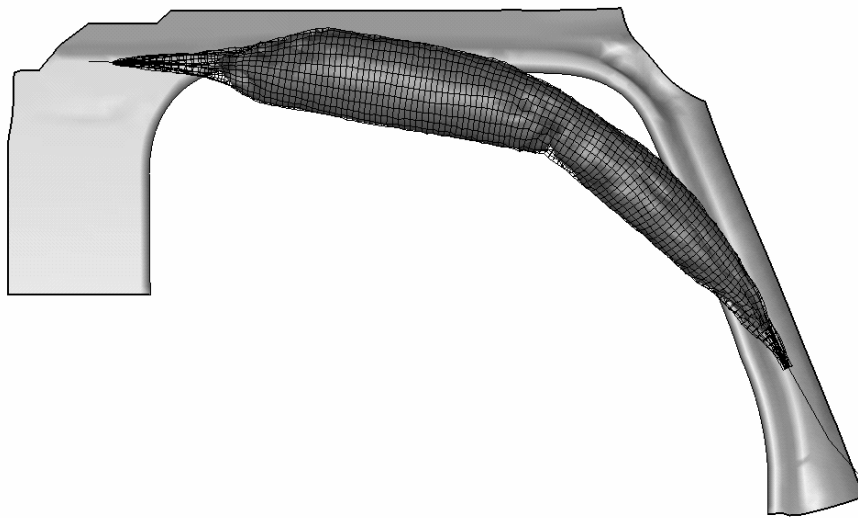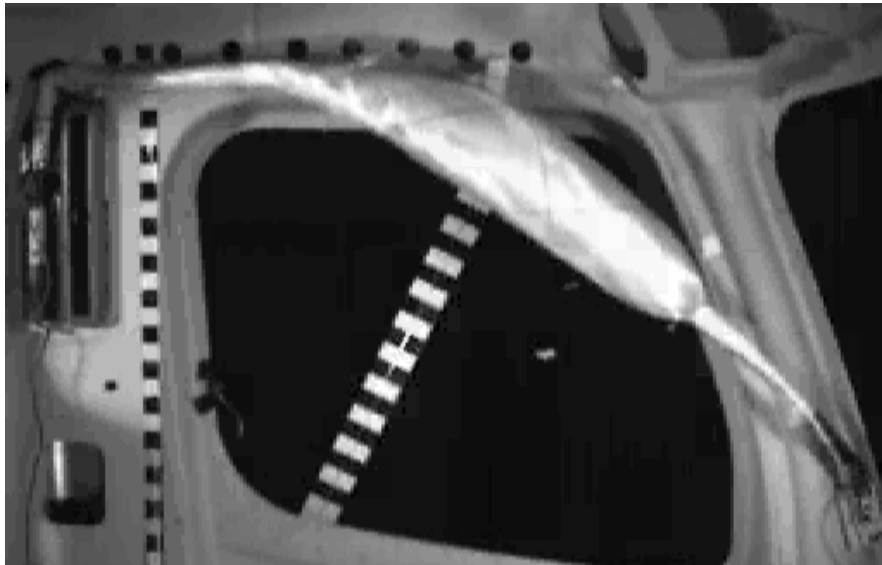
Figure 9. Test and FE Analysis at $t = 10$ ms
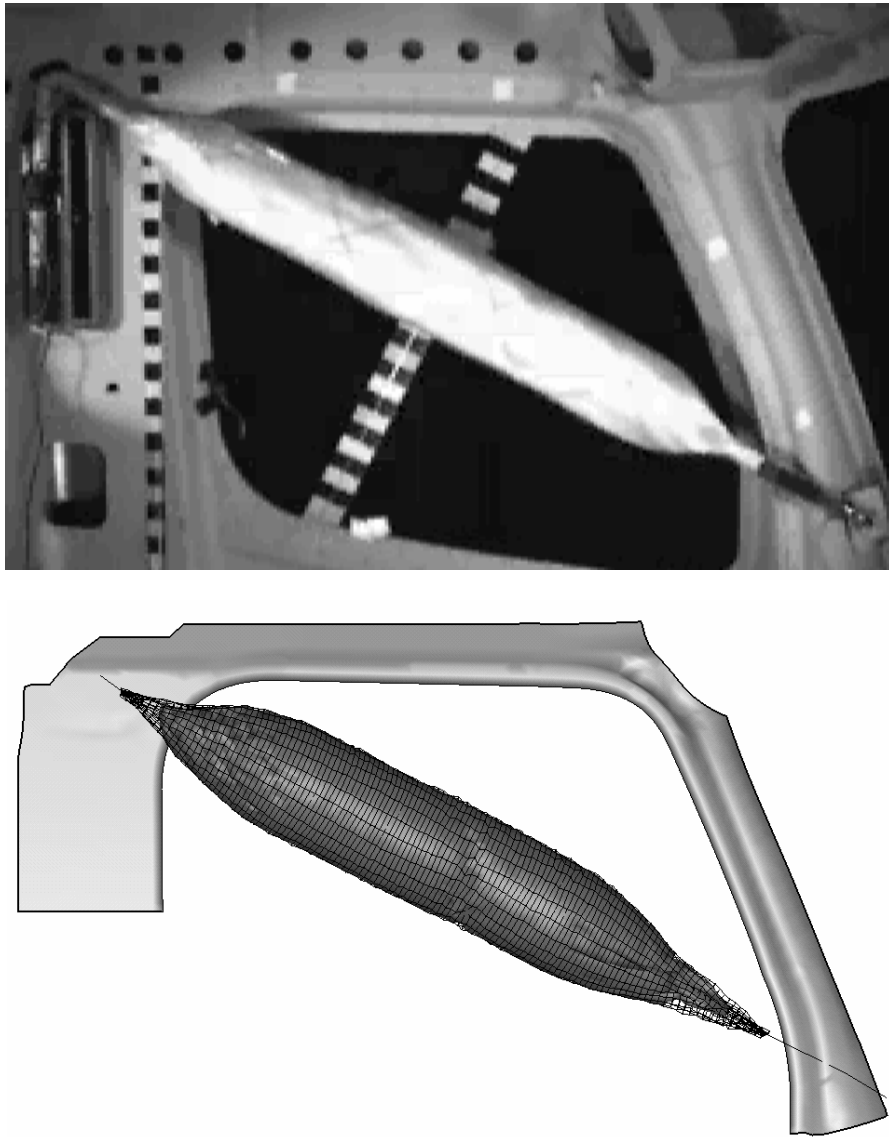
Figure 10. Test and FE Analysis after Full Inflation

To illustrate the performance of the FE model, results from the analysis are presented here and are compared to the test results. Figs. 8–10 show the inflatable structure at different stages of inflation. Although both inner and outer bags are modeled using shell finite elements, on the figures the outer bag is represented by a wireframe in order to make the inner bag visible.

Fig. 11 shows the shape of an element before the airbag is inflated and after full inflation. As seen, the element undergoes a significant deformation as the weft and warp fibers in the LWF layer reorient and the angle between them changes. Fig. 12 displays the variation in time of the pressure inside the inner bag for the test and the FE analysis. The significant initial jump of the test pressure is due to the fact that it is measured in the vicinity of the inflator outlet orifice, is partly a measure of stagnation pressure and not static pressure, and therefore it would not accurately represent the pressure inside the bladder prior to its uniform distribution. As seen from the curves, after the pressure in the bag settles to a relatively uniform spatial static pressure distribution, the values of the test and analysis curves get quite close.

Fig. 13 shows the variation in time of the force in one of the straps anchoring the system to the cab body. Although there is some discrepancy in the initial values, the curves are quite close for most of the inflation time. As seen, both

the force value and its frequency of oscillation are captured very well by the FE model. The variation in time of the angle between the weft and warp fibers is presented on Fig. 14. Starting from 46°, these fiber reorient as the airbag inflates to be almost orthogonal at full inflation. All curves on Figs. 12–14 represent data after filtering to SAE Class 60.

Time = 0, α = 46°   Time = 0.1, α = 96°
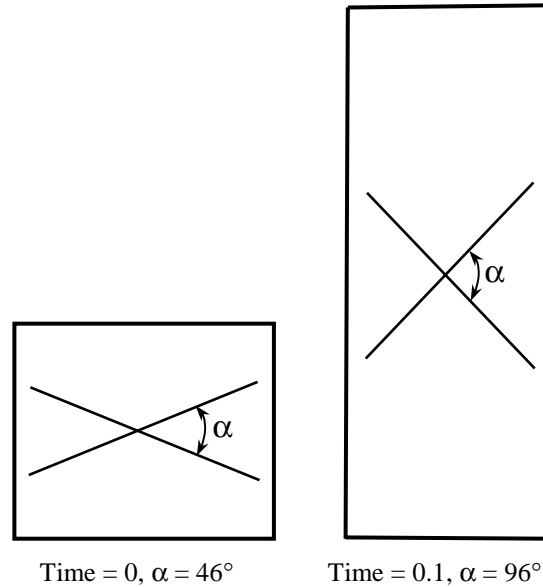
Figure 11. Element Shape and Fibers Orientation Before and After Inflation
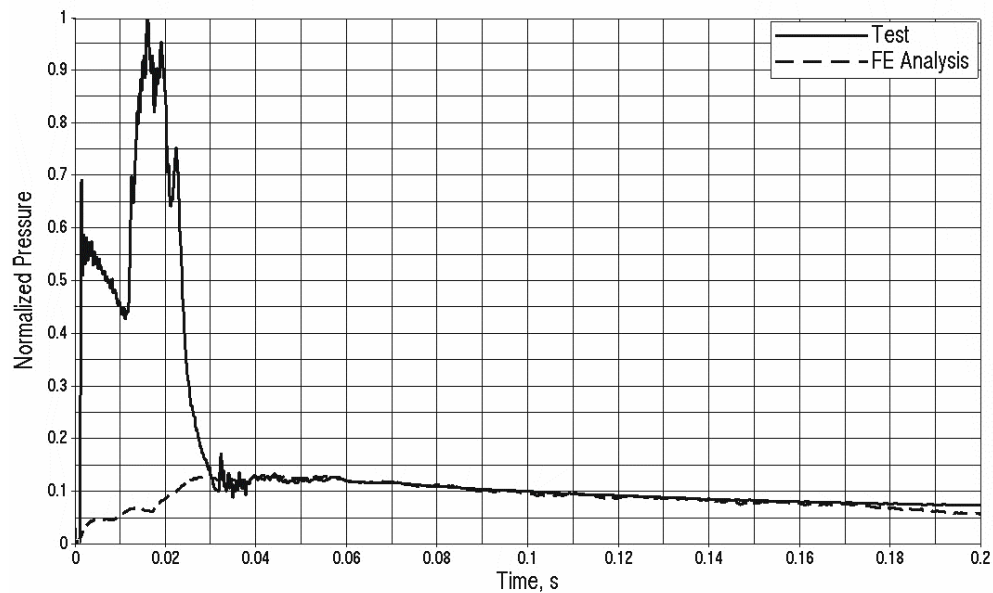
Figure 12. Pressure Variation in Time within the Inner Bladder

The results acquired show the excellent performance of the FE model and the loosely woven fabric material formulation in particular. They build confidence in the capabilities of the developed material model to accurately and efficiently represent loosely woven fabric layers within a finite element analysis scheme.
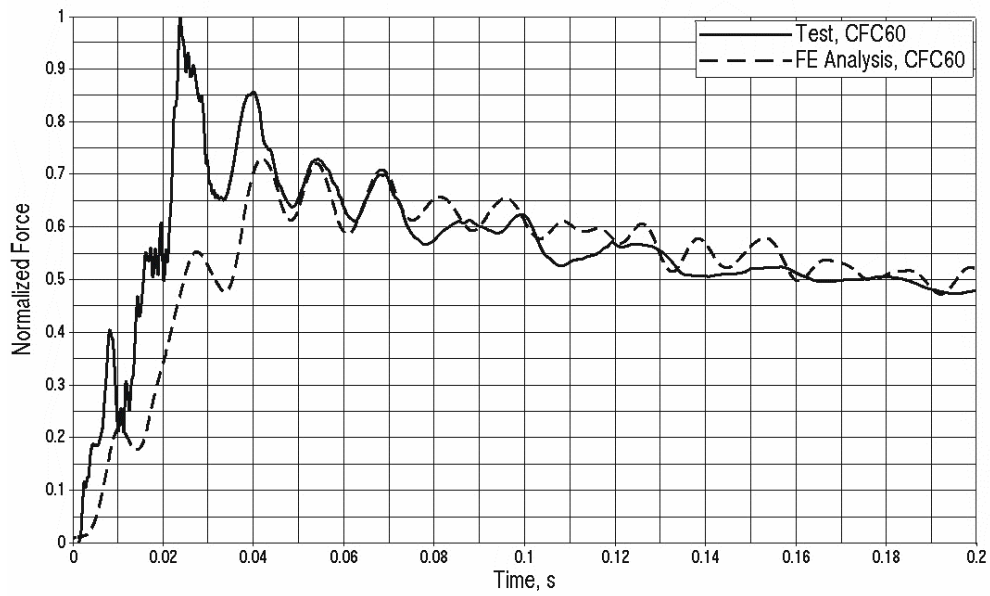
Figure 13. Strap Force Variation in Time
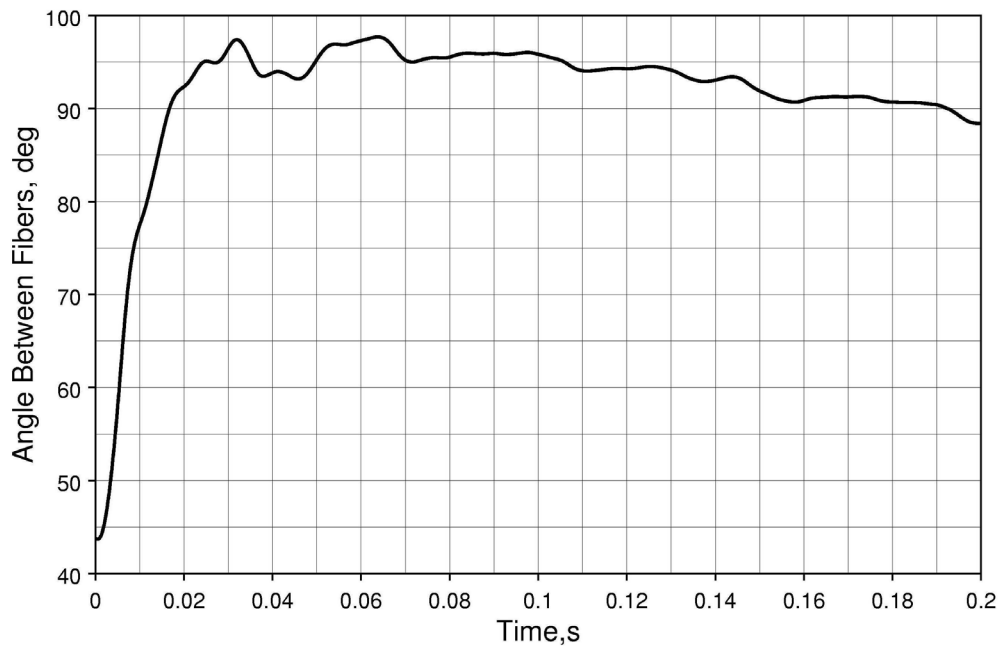
Figure 14. Angle between LWF Fibers Variation in Time

CONCLUSIONS

With its unique capabilities to model the behavior of loosely woven fabrics with nonorthogonal fibers and changing fiber angles during the deformation, the newly developed model contributes to the analysis capabilities of the FE constitutive models library. Its simple and efficient formulation and implementation makes it very attractive for explicit FE schemes used in vehicle occupant protection and crashworthiness simulations. Its good accuracy and reliable performance make it an excellent and unique tool for the analysis of some recently developed advanced occupant protection systems.

REFERENCES

BATHE, K.-J. (1996). Finite Element Procedures, Prentice-Hall, Inc., Englewood Cliffs, New Jersey, USA, p. 507.

HALLQUIST, J.O. (1998). "LS-DYNA Theoretical Manual", Livermore Software Technology Corporation, Livermore, CA.

ISHIKAWA, T. and CHOU, T.W. (1982). "Stiffness and Strength Behaviour of Woven Fabric Composites", Journal of Materials Science, 17, pp. 3211–3220.

MEISTER, M. and STEENBRINK, S. (1999). "Modelling of Loosely Woven Fabrics for ITS Airbag Simulations", 2nd European MADYMO User's Conference, Stuttgart, May 28.

NAIK, N.K. and GANESH, V.K. (1995). "An Analytical Method for Plain Weave Fabric Composites", Composites, 26, pp. 281–289.

TABIEI, A., JIANG, Y., and YI, W. (2000). "Novel Micromechanics-based Woven-fabric Composite Constitutive Model with Material Nonlinear Behavior", AIAA Journal, 38(8), pp.1437–1443.

TANOV, R. and TABIEI, A. (2001). "Computationally Efficient Micromechanical Woven Fabric Composite Elastic Constitutive Models", Journal of Applied Mechanics, 68, pp. 553−560.

TNO AUTOMOTIVE (1999). MADYMO Theory Manual Version 5.4, TNO Automotive.

WHITCOMB, J., SRIRENGAN, K., and CHAPMAN, C. (1995). "Evaluation of Homogenization for Global/Local Stress Analysis of Textile Composites", Composite Structures, 31(2), pp.137–149.